A STUDY OF FISSION YIELDS USING A HIGH SENSITIVITY MASS SPECTROMETER

A STUDY OF FISSION YIELDS USING A HIGH SENSITIVITY MASS SPECTROMETER

by

TERENCE JAMES KENNETT, B.Sc.

A Thesis

Submitted to the Faculty of Arts and Science

in Partial Fulfilment of the Requirements

for the Degree

Master of Science

McMaster University

October 1954

MASTER OF SCIENCE (1954) McMASTER UNIVERSITY
(Physics) Hamilton, Ontario

TITLE: A Study of Fission Yields Using A High Sensitivity Mass Spectrometer

AUTHOR: Terence James Kennett, B.Sc. (McMaster University)

SUPERVISOR: Dr. H. G. Thode

NUMBER OF PAGES: v, 28, 10 figures

SCOPE AND CONTENTS:

An electron multiplier has been developed which has increased the sensitivity of an existing mass spectrometer by a factor of 10^5. This increased sensitivity has permitted determination of fission yields of substances that have undergone little fission. Two such samples, for which the rare gas isotopes have been analysed, are Bohemian pitchblende and the products resulting from the neutron fission of Th^{232}.

The Bohemian ore exhibited more neutron fission than any uranium deposit previously analysed. An explanation of this effect may be obtained by consideration of the geological and chemical nature of the deposit. The neutron fission of thorium, which shows fine structure in both the xenon and krypton regions, is similar to the patterns of U^{235}, U^{238} and Pu^{239}.

ACKNOWLEDGEMENTS

The author wishes to thank Dr. H. G. Thode for his continuing interest and direction throughout this investigation. He is also indebted to Dr. C. C. McMullen for his generous assistance and advice and to Dr. W. H. Fleming for many interesting and helpful discussions.

The chance to pursue this investigation was made possible by the generous financial assistance of the Research Council of Ontario.

TABLE OF CONTENTS

LIST OF ILLUSTRATIONS

INTRODUCTION

In recent years neutron induced fission and spontaneous fission of heavy nuclei have been under extensive study. The investigation of neutron fission has been primarily directed towards U^{235}, while pitchblende ores have yielded spontaneous fission results. Earlier work indicated a smooth asymmetrical mass-yield curve; however, later results have shown deviations or fine structure along the curve. Mass spectrometric analyses of krypton and xenon fission yields have indicated fine structure in both regions. The sensitivity of a mass spectrometer built here previously has been increased considerably by the use of an electron multiplier, so that fission yields of samples that have undergone little fission can be determined with it. Accordingly, determination of the fission yields of Bohemian pitchblende and neutron fission of Th^{232} were undertaken.

The spontaneous fission of uranium was first reported in 1940 (1), and since then a number of attempts have been made to determine the fission half-life. Segrè (2) has reported the spontaneous fission half-life of the isotopes of uranium, and the values given for U^{238} and U^{235} are respectively $8.04 \pm 0.3 \times 10^{15}$ and $1.87 \pm 0.6 \times 10^{17}$ years. Macnamara and Thode (3) reported the xenon and krypton fission patterns for uranium

minerals and concluded that spontaneous fission was involved. While their results indicated an asymmetric mass-yield curve similar to thermal neutron fission of U^{235}, the curves were steeper and the xenon to krypton ratio was larger. Both these facts suggest that spontaneous fission was involved. Fine structure in the mass yield curve was evident from the high yield of Xe^{132}. Analysis of U^{235} + n has shown a high Xe^{133} and Xe^{134} yield so the shift to lower masses suggests spontaneous fission of U^{238}, since the Glendenin mechanism (4) accounts qualitatively for such a shift.

Fleming and Thode (5), and others (6) have reported the xenon and krypton yields for a group of uranium ores including a sample of uraninite. They found the fission yields, as well as the fine structure of Xe^{132} and Xe^{134} varied markedly between pitchblendes, indicating varying proportions of spontaneous and neutron fission. The amount of each type of fission was found to be dependent on the uranium concentration, geological age, and the impurities in the mineral.

The discovery of neutron fission was made by Hahn and Strassmann (7) in 1939. Since then the general asymmetric fission yield curves for U^{233}, U^{235}, U^{238} and Pu^{239} have been fairly well established; however, the fundamental nuclear data pertaining to the neutron fission of Th^{232} are rather meager. Thermal neutrons apparently cause no observable fission and the cross-section only reaches detectable values (8) for neutron energies of 1.10 ± 0.05 Mev. Turkevich and Niday (9) have re-

ported the relative yields of twenty-three fission yield chains for Th^{232} fission using radio-chemical methods. Although these results are small in number and have rather large errors, they are sufficient to characterize the mass yield curve which is shown in figure 1.

Mass spectrometric and β^- counting experiments have indicated fine structure on the smooth fission yield curves of plutonium and the uranium isotopes. An attempt to explain these abnormal yields has been made by Glendenin (10) and elaborated on by Pappas (11). This model assumes that primary fission products containing 1, 3, 5 and 7 neutrons in excess of a closed shell will undergo neutron emission in addition to β^- decay. Any method of predicting the fine structure involves the nuclear charge distribution in fission.

The nuclear charge distribution is given by the following equation, in which Th^{232} captures a neutron and undergoes fission.

$$Th^{232} + n \longrightarrow \left[{}_{90}Th^{233}\right]^{*} \longrightarrow {}_{Z_1}A_1 + {}_{Z_2}A_2 + \nu n + Q + \gamma$$

The A and corresponding Z represent the mass and atomic number respectively of the primary fission products; ν is the average number of neutrons emitted per fission, Q the kinetic energy of the fragments (ca 200 Mev) and γ the prompt gamma ray energy. By concervation laws it is assumed $A_1 + A_2 + \nu = 233$ and $Z_1 + Z_2 = 90$. The neutron to proton ratio is higher for the heavy nuclei in which fission is observed than for stable nuclei of the medium masses which are produced by the fission process. The

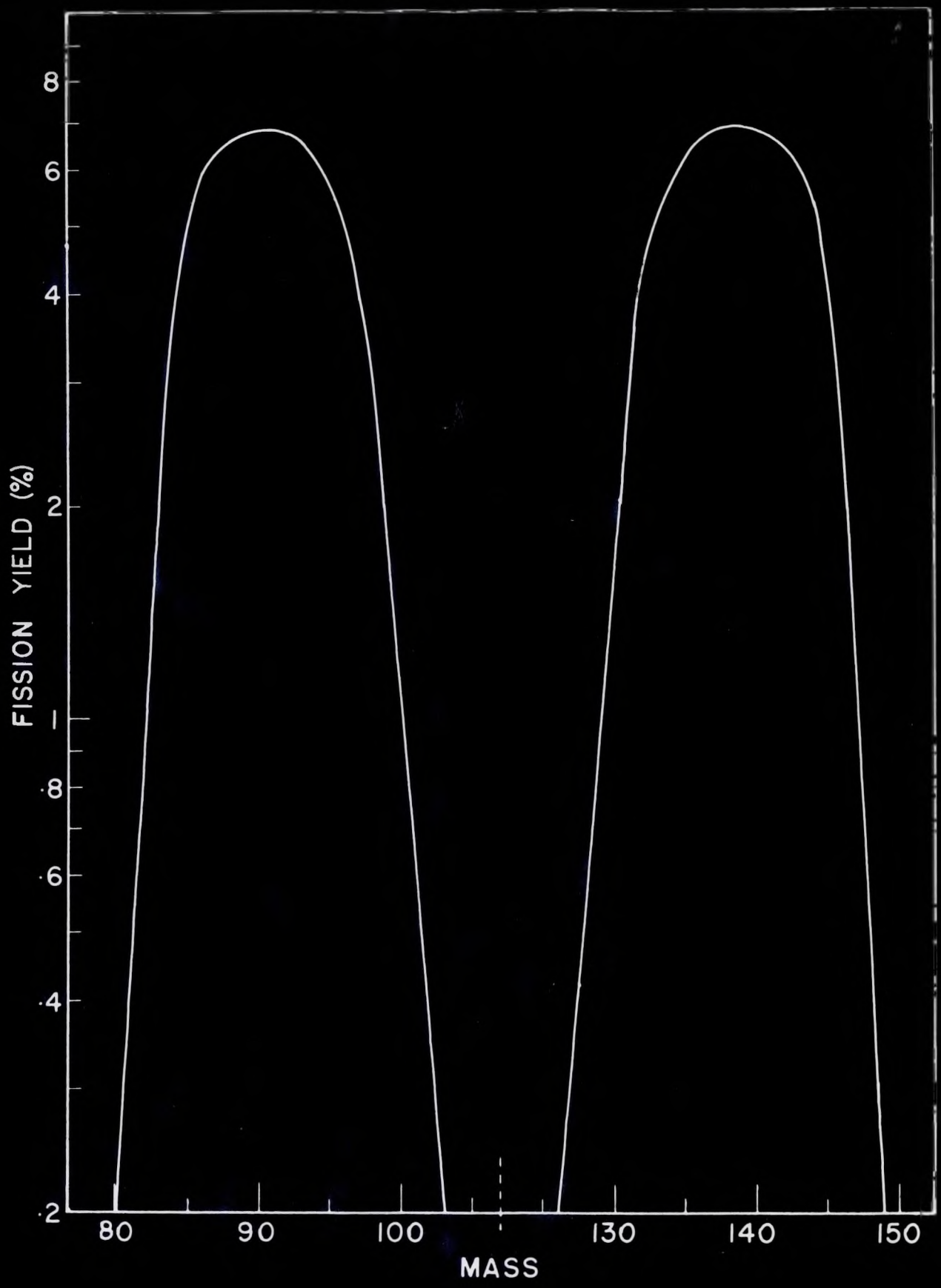

RADIOCHEMICAL FISSION YIELD CURVE. (9)

FIGURE 1.

fission fragments will therefore have too large a neutron excess and be unstable towards β^- decay. Beta decay increases the atomic number by one and leaves the mass number constant, hence the neutron excess is reduced. In general the average primary fission product undergoes approximately three β^- decays and releases about 11 Mev. before nuclear stability is achieved.

It is important to know which member of a particular fission chain has the greatest probability of being a primary fission product. This involves finding the most probable primary charge Z_p for a given mass number A and also how the probability is distributed around Z_p. Glendenin (10) has found empirically from U^{233}, U^{235}, and Pu^{239} results that the most probable mode of charge division is that which leads to equal charge displacements. This implies that the effective chain lengths for the two primary fission products are equal. The value of Z_p is found by the relation

$$Z_p = Z_A - \tfrac{1}{2}(Z_A + Z_{233-A} - 90)$$

where Z_p is the most probable charge for the given mass chain A-1 since a neutron is assumed to be emitted by each fragment after fission. Z_A is the most stable charge for a nucleus of mass A as determined by Bohr and Wheeler (12) and revised recently by Coryell (13). The probability for the formation of a nucleus of mass number A and charge Z as a primary fission product is shown in figure 2.

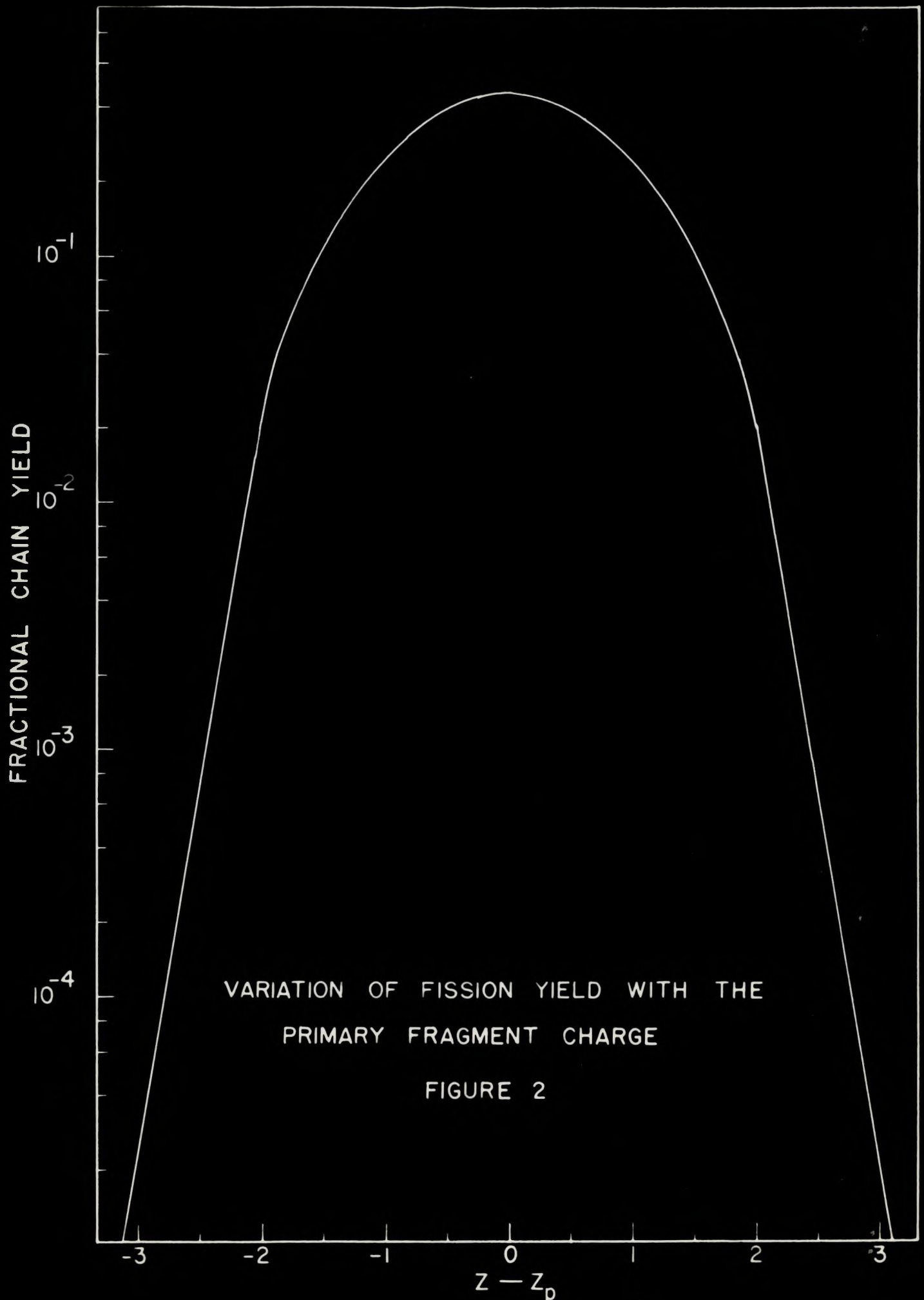

VARIATION OF FISSION YIELD WITH THE PRIMARY FRAGMENT CHARGE

FIGURE 2

EXPERIMENTAL

APPARATUS

Theory. Secondary emission of electrons resulting from the bombardment of metallic surfaces with protons was first reported by Healea and Chaffee (14), in whose experiments 1600 ev. protons were made to impinge on a nickel target. Allen (15) continued this work using 48 to 212 kev. protons and a variety of target materials. Of the metals investigated, beryllium and copper were found to yield the greatest secondary emission. The first electron multiplier developed (16) employed beryllium plated dynodes and when installed in a mass spectrometer, some low mass ions were detected. Cohen (17) used this type of multiplier to search for new isotopes of cerium. More recently Inghram and Hayden (18) have done a considerable amount of research on the application of electron multipliers to mass spectrometry.

The principle of the electron multiplier is similar to that of the photomultiplier; the only distinction being that ions rather than photons are detected. Ions impinging on the first or conversion dynode eject secondary electrons which are accelerated and focused on to the next dynode. This process continues down the dynode chain with an increasingly large number of electrons participating until they reach the final dynode or grid where they are collected. Thus the electron multiplier converts an ion

current to a considerably larger but nevertheless proportional electron current.

Description. The structure of the multiplier which has been used is a half scale modification of Allen's (19) linear electrostatically focussed design and is shown in figure 3. Since it was desirable to mount the multiplier in a conventional mass spectrometer tube, the conversion dynode had to be reshaped and re-orientated so that the ion beam could be parallel to the axis of the dynode assembly. The dynodes, which are fabricated from .0071" CuBe (2% Be) sheet, are mounted between two lavite plates which serve as insulating locators. The first three dynodes are electrically shielded to reduce noise and the whole structure is held rigidly by three mounting rods. The manner of assembly ensures an accurate line up between the defining slit and conversion dynode. The voltage divider network, which consists of a series of one megohm resistors, is located outside the tube because of space limitation.

To obtain the maximum gain from a multiplier, it is necessary to activate the dynodes. Activation can be achieved by heating the plates under reduced pressure in air or in an atmosphere of hydrogen or argon. The following procedure, using hydrogen, was found to be comparable to other processes (20). The dynodes were cleaned abrasively and then placed in a hydrogen furnace. The furnace temperature was gradually increased to 650°C, held there for fifteen minutes and then allowed to cool. Once the multiplier has been activated, exposure to atmospheric pressure does not appear to reduce the gain appreciably.

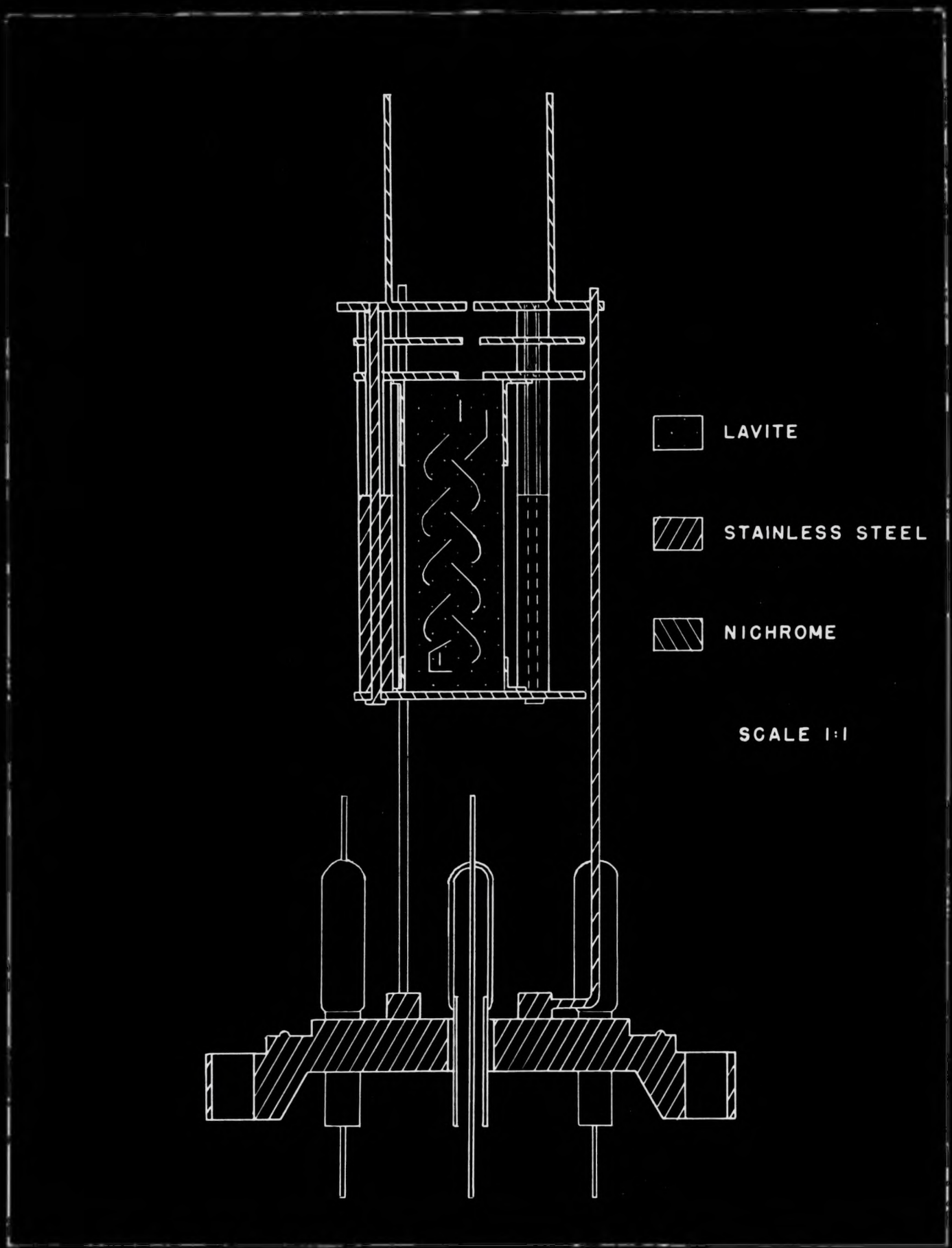

FIGURE 3

In mass spectrometry the resultant signal due to an impinging ion beam must be large compared to the fluctuations in the recorder base line at no input signal. The fundamental limitation of the multiplier itself is the dark current which can be minimized by careful design of the multiplier (21).

The collector system in both the multiplier structure and the external circuit must be designed so as to minimize ohmic leakage. If present this leakage may cause not only a varying d.c. component but also spurious pulses due to rapid fluctuations. The present design is susceptible to leakage because of its reduced dimensions. The effectiveness of the high resitivity of lavite is reduced because of the proximity of the dynodes. The design of Inghram (20) in which the dynodes are supported by lavite rods rather than plates appears to afford much greater protection against leakage.

The existance of a direct path between input and output within the tube permits the possibility of maintaining a continuous current flow within the multiplier with no external excitation due to ion feedback. If the pressure in the collector region is large the residual gas may be ionized by the electrons as they follow their normal paths through the multiplier. The positive ions so formed will tend to travel backwards towards the input due to the voltage gradient. If they strike an active surface secondary electrons will be produced, thus a positive feedback link will be established. If this occurs the currents become excessive and the multiplier goes into continuous dis-

charge. This undesirable condition is best overcome by having a very low pressure in the multiplier region and can be attained by pumping directly from the collector end of the tube.

Field emission will occur at the surface of a conductor if the potential gradient is sufficiently large. Therefore the multiplier must be designed so as to minimize potential gradients and to eliminate any sharp edges or projections from components at high potential. Thermionic emission is a fundamental limitation determined by the absolute temperature and the work function of the dynode material.

Operation. Any study of the properties of an electron multiplier is very complex since numerous phenomena are involved. The principal processes to be considered are (18):

(a) the energy of the incident particle,

(b) the mass of the incident particle,

(c) the electronic configuration of the incident particle,

(d) the charge of the incident particle,

(e) the chemical and physical composition of the surface,

(f) the angle at which the incident particle strikes the surface.

The properties of the electron multiplier which are of most importance in mass spectrometry are mass response and the dependence of gain on dynode and ion voltages. The gain was determined for the isotopes of normal xenon and for elements of widely differing mass. All possible voltage parameters were varied in order to find the effect of each on the overall gain.

The voltages on the multiplier are arranged so that the collecting grid is near ground potential. This eliminates the need for the amplifier to be operated at high potential. For positive ions there is an additional advantage of this arrangement in that the voltage across the multiplier is added to the energy of the ion beam, thus increasing the multiplication of the first stage. Figure 4 shows the dependence of gain on ion energy for a constant voltage per stage on the multiplier, for several values of voltage. The graph also shows how the multiplier responds to different masses and electronic configurations. There appears to be a threshold energy depending on mass below which no secondary electrons can be initiated. The slope of curves having constant dynode voltage is independent of mass and it is possible to write:

$$G = aV_E + b$$

for the gain G where V_E is the total energy of the ions, a is a function of the voltage per stage and b depends on the A and Z of the incident ions. The curves for constant V_s indicate that mass discrimination decreases with increasing mass. Since the multiplier voltage, 10 V_s, is added to the source voltage V_a then

$$G = a(V_a + 10V_s) + b$$

The nature of the multiplication process can be mathematically represented by

$$G = G_1(G_2)^9$$

where G_1 is a function of ion energy and mass, and G_2 is a

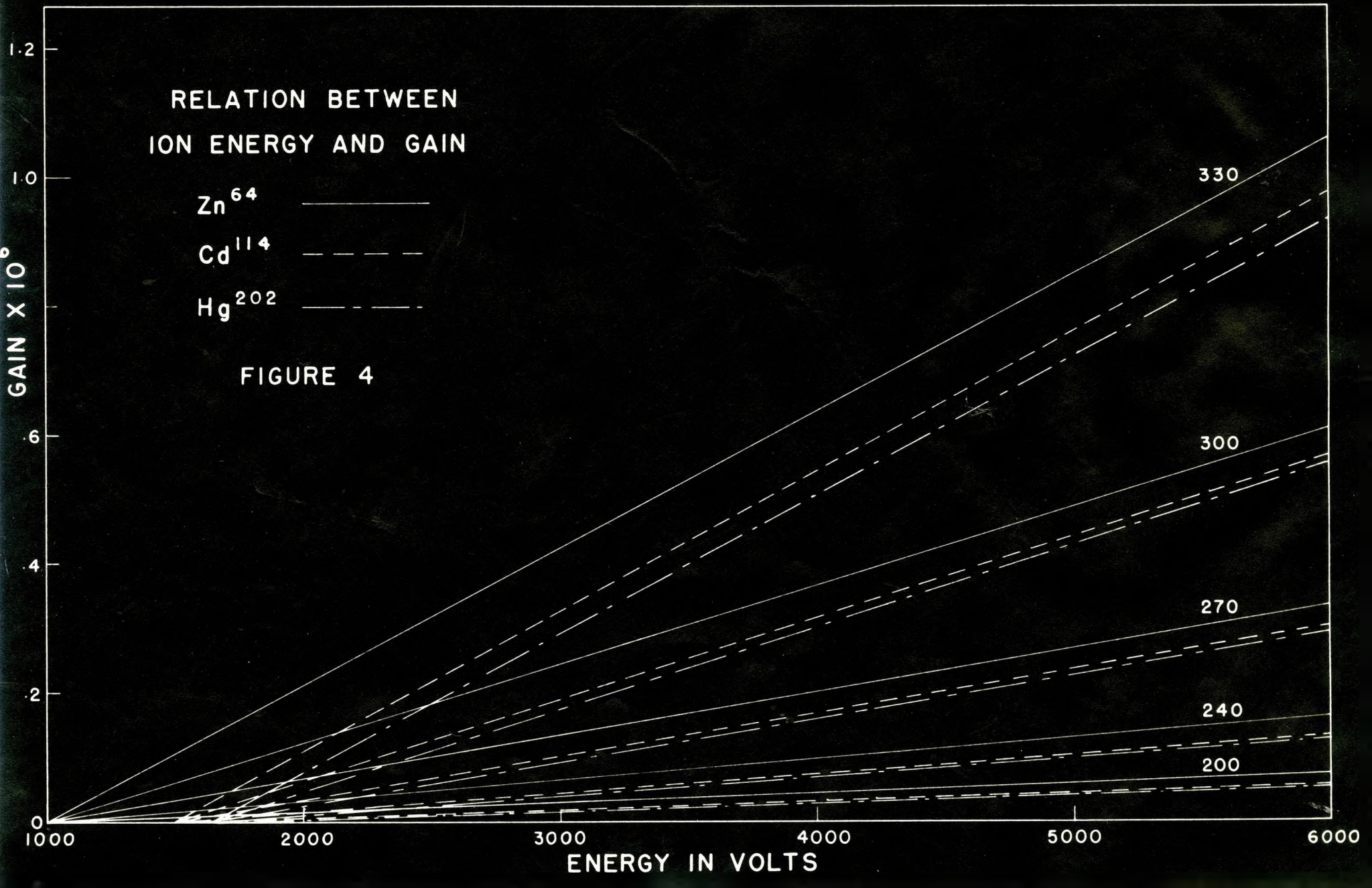
RELATION BETWEEN
ION ENERGY AND GAIN
Zn 64
Cd 114
Hg 202
FIGURE 4
GAIN X 10⁶
1.2
1.0
.6
.4
.2
0
330
300
270
240
200
1000
2000
3000
4000
5000
6000
ENERGY IN VOLTS

function of V_s only. Figure 5 which is essentially a transfer characteristic of figure 4 shows the dependence of gain on V_s for a constant ion energy. Since the mass and energy of the ions are fixed G_1 is a constant so that the curve is actually $(G_2)^9$ against V_s. The rapid increase of gain with V_s due to the exponential nature of the G_2 term illustrates the need for high stability of the multiplier voltage. The value $\partial G/\partial V_s$ equals 10^4 for $V_s = 300$ volts indicates a stability of one part in 50,000 for satisfactory operation. The general shape of the curve shows that large gains are limited by the stability of V_s.

If the curves in figure 5 which are represented by $G = G_1(G_2)^9$ are divided by G_1 and the ninth root taken it is then possible to find the relation between G_2 and V_s. A plot of this function is shown in figure 6 and represents the dependence of secondary emission on the energy of the impinging electron. The curve is very nearly linear in the region 190 to 330 volts and by the method of least squares can be represented by

$$G_2 = I_s/I_p = .0097V_s + 1.11$$

This function is of course independent of the incident particle.

The mass spectra obtained for samples of the order of a cubic millimeter were similar to those of a simple collecting instrument. However, for samples of 0.01 cmm. quite different spectra were obtained as shown in figure 7. The gain of the multiplier in the xenon region was about 10^5 and with the amplifying arrangement used a 10 mv. signal was equivalent to

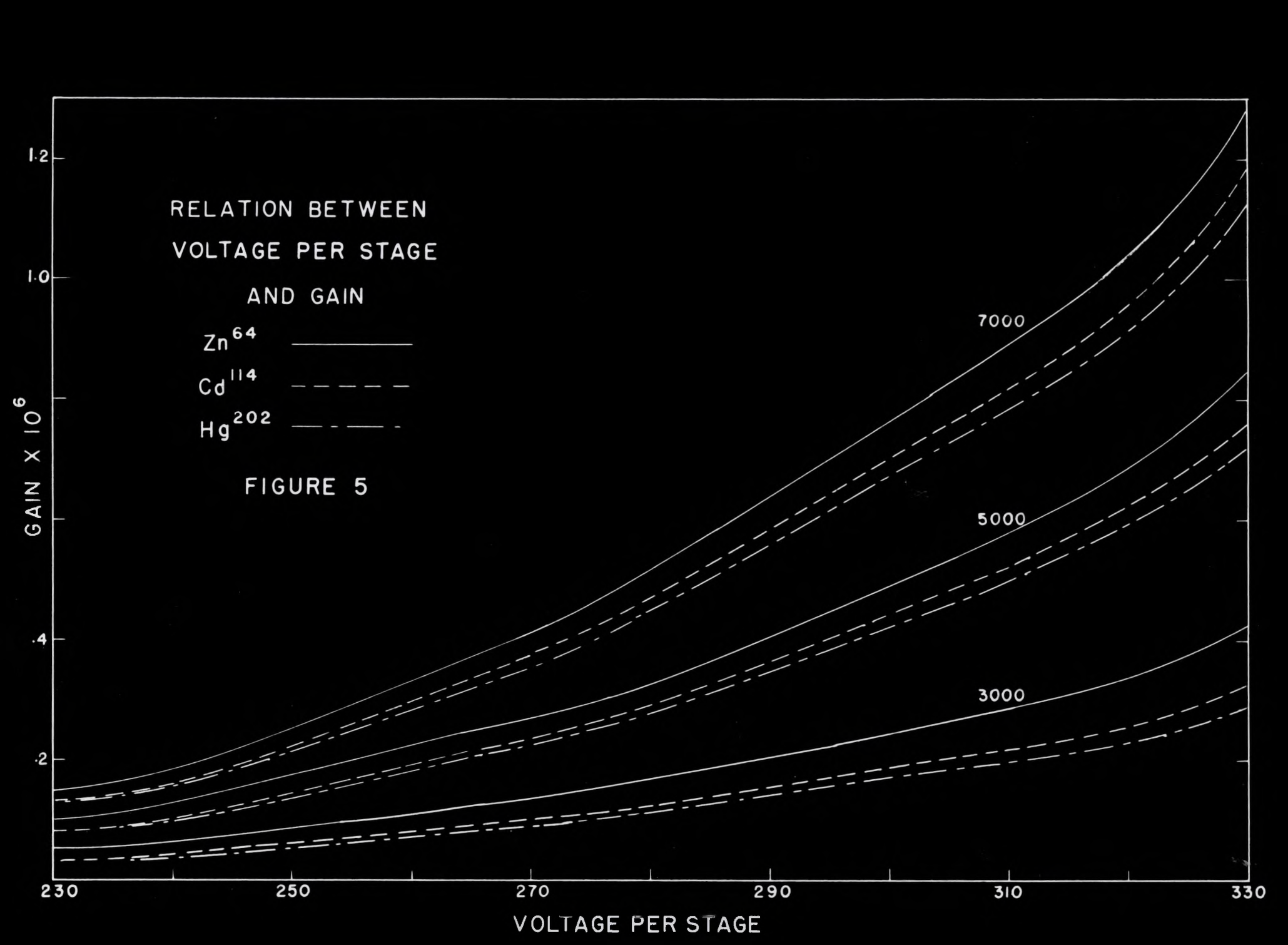
RELATION BETWEEN
VOLTAGE PER STAGE
AND GAIN
Zn64
Cd114
Hg202
FIGURE 5
7000
5000
3000
1.2
1.0
.4
.2
GAIN X 10^6
230
250
270
290
310
330
VOLTAGE PER STAGE

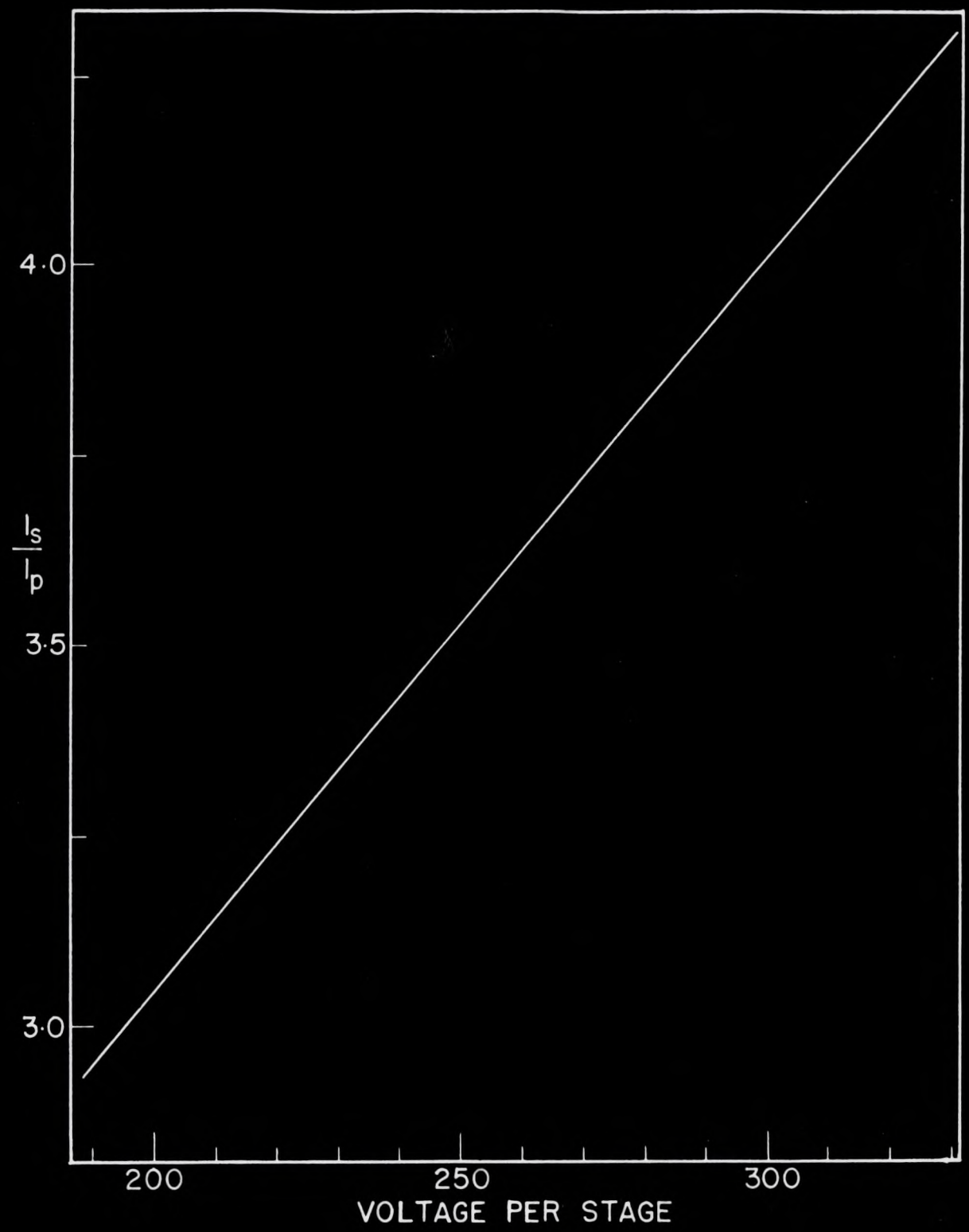

SECONDARY ELECTRON YIELD CURVE

FIGURE 6

20,000 ion/sec. A peak of 10 mv. was found to have a noise or jitter on the top of 1 mv. or 2,000 ions/sec. The per cent noise appears to be a function of the ion current as shown in figure 7. The jitter is larger by a factor of five than would be expected if a Guassian distribution was assumed for the ion current. The base line between peaks is very flat indicating little noise in the detecting system so that the jitter can only be associated with the ion current and its magnitude. The possibility of statistical variation is quite large if only one out of n ions striking the conversion dynode produces secondary electrons. In such a case the statistical fluctuations would be increased by a factor of $\sqrt{n}$.

If this is a statistical process there is a simple method for measuring the relative gain for different masses. For a statistical relation the percent jitter j must be proportional to $1/\sqrt{n}$, where n is the number of ions per second. Therefore if two masses produce the same signal then

$$G_1 n_1 = G_2 n_2$$

$$\text{and } j_1 = k/\sqrt{n_1}, \qquad j_2 = k/\sqrt{n_2}$$

$$\text{then } j_1/j_2 = \sqrt{n_2/n_1}, \text{ so that } n_1/n_2 = (G_1/G_2) = (j_1/j_2)^2$$

This relationship was tried for Zn^{64} and Cd^{114} using several different ion currents and was found to agree with the results shown in figure 4. The agreement implies that the jitter is statistical in nature and therefore cannot be easily reduced. The large gain of the multiplier permits the use of small grid

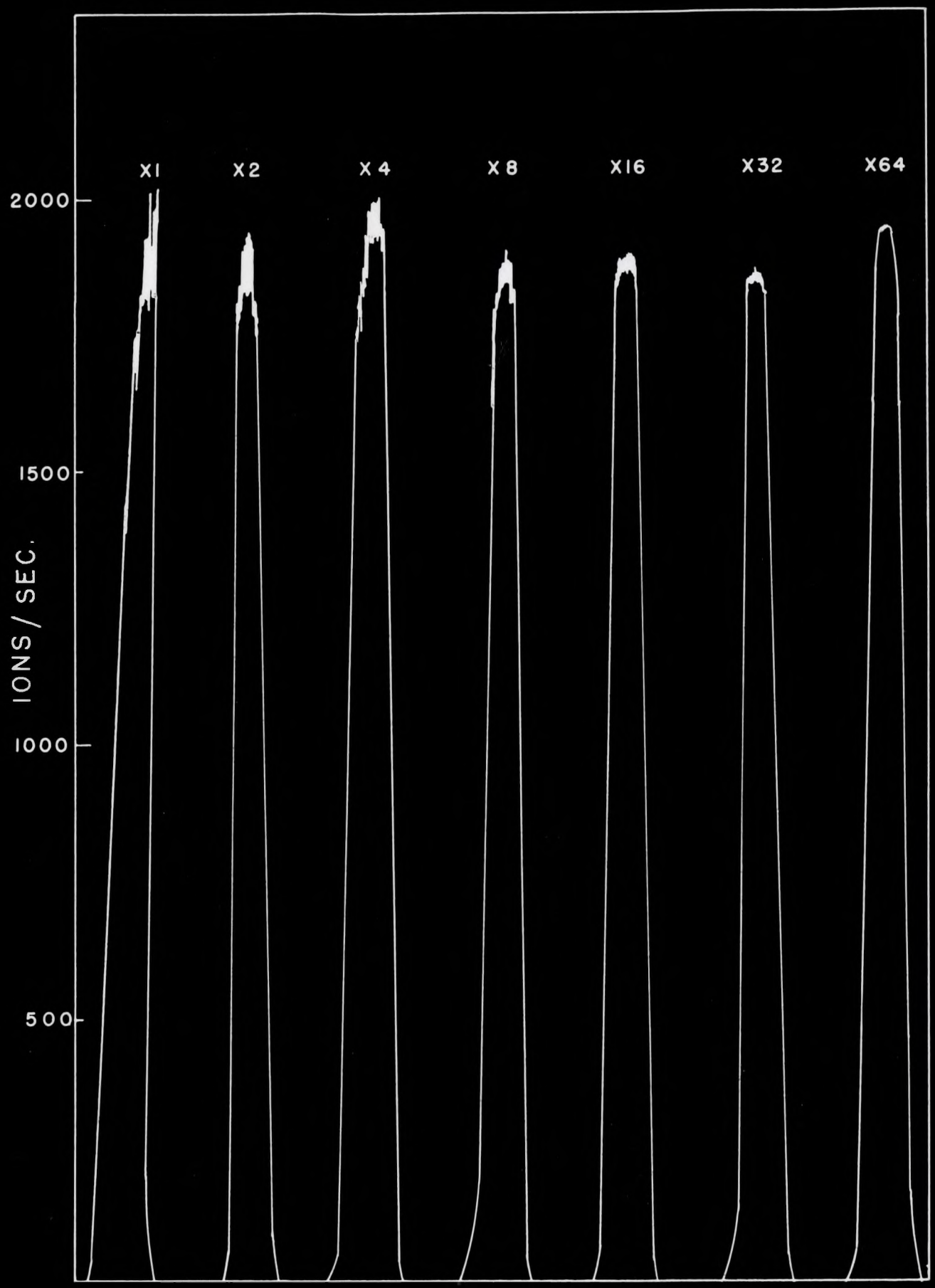

FIGURE 7

leaks which speed up the circuit response considerably. To detect the first peak in figure 7 a single collecting instrument would require a factor of 10^4 increase in grid leak hence the large time constant would hide the effect entirely. While the rapid fluctuations limit the size of measurable peaks it is possible to detect currents of 10^{-17} amperes or about 60 ions per second.

The problem of accuracy in the measurement of peaks corresponding to small ion currents was investigated by studying the abundances of fission product xenon. By considering the first peak in figure 7 it is seen that two values for the peak height are possible; the maximum or an estimated mean can be taken. Both methods yield comparable results as shown in Table I.

TABLE I

Estimate of True Peak Height Using Xe Fission Yields (%)

	131	132	134	136
Max. Height	3.28	4.88 ± .02	8.90 ± .01	6.99 ± .03
Ave. Height	3.28	4.89 ± .02	8.93 ± .02	7.02 ± .02
Single Coll.	3.28	4.91 ± .02	8.98 ± .02	7.08 ± .02

The mean height measurements yield results which agree a little more closely with the single collection values than do the maximem results. Because of this agreement and also the assumption of a statistical process the mean height has been used for all

results recorded in this thesis.

Mass Spectrometry. The nearly monoergic beam of ions leaving the source passes through the sector magnet, is bent and dispersed in a spectrum according to the mass to charge ratio of the constituent ions as shown by the equation:

$$e/m = 2V/H^2R^2$$

To measure the intensity of a particular type of ion, the ratio of the magnetic field strength to ion energy is adjusted until they pass through the slit in front of the electron multiplier. The slit width is such that nearly all the ions in question will pass through to the exclusion of those having different charge to mass ratios. The current from the multiplier is fed to an Allied Physics Corporation vibrating reed electrometer where it is amplified; the output goes to a Leeds and Northrup Speedomax recorder so that a permanent record is obtained.

The performance of the electron multiplier was studied using a 10" single focusing sector type mass spectrometer. An electron bombardment source was used and the scanning was entirely magnetic. A pressure of 5×10^{-8} mm. of mercury was found necessary for satisfactory operation of the electron multiplier. To obtain this pressure the pumping system consisted of a three-stage glass mercury diffusion pump backed by a Welch Duo-Seal fore pump. A liquid-air trap was installed between the diffusion pump and mass spectrometer to trap out mercury and other vapours. A dry-ice trap was used between the diffusion and fore pump to minimize hydrocarbon residuals. The

pumping speed of the system was approximately 80 litres per second. A furnace was wrapped on the mass spectrometer tube so that the entire system could be baked at a temperature of 400°C.

SAMPLE PREPARATION

Bohemian Pitchblende. The method and apparatus for extracting rare gases from uranium has been described elsewhere (24) and only a slight modification is necessary for application to pitchblendes. The ore is ground and dissolved in sulfuric acid; the released gas is passed through a chemical drying train including an ascarite trap to absorb CO_2 which is released from carbonates associated with the pitchblende. A simple calcium furnace is used after the drying train for the initial purification of the rare gas sample. Final purification consists of repeated calcium furnace treatments until the volume which is measured in a McLeod gauge remains constant.

Thorium Metal. The thorium was dissolved in a saturated solution of cupric potassium chloride which is the same method used for uranium (24). The fission product rare gases which are liberated pass through a purification process similar to that described for pitchblende samples.

RESULTS AND DISCUSSION

Mass Discrimination. In mass spectrometry where relative abundances are to be determined it is necessary to know and correct for any mass discrimination. The response to various elements of differing mass is shown in figure 4; however, the response to the isotopes of a particular element is of greater importance. Table II contains the relative abundances of normal xenon as measured using a Faraday cup as a single collector and the electron multiplier. The values reported by Nier (23) have been corrected for mass discrimination by calibration with known isotopic mixtures. The last column of results are those obtained using a 180° simple collecting mass spectrometer.

TABLE II

Percent Abundances of Normal Xenon

Isotope	Single Coll.	Multiplier	Nier	180°
128	1.87 ± .01	1.94 ± .01	1.92 ± .01	1.84 ± .02
129	26.22 ± .02	26.64 ± .02	26.44 ± .08	26.26 ± .08
130	4.03 ± .01	4.10 ± .01	4.08 ± .01	4.03 ± .02
131	21.18 ± .05	21.19 ± .02	21.18 ± .07	21.29 ± .08
132	27.00 ± .06	26.79 ± .04	26.89 ± .07	27.14 ± .08
134	10.50 ± .03	10.40 ± .01	10.44 ± .02	10.43 ± .02
136	8.98 ± .01	8.77 ± .01	8.87 ± .01	8.86 ± .01

The results represent an integrated effect of discrimination in the leak, source and collector. The first column indicates a better response to higher masses for single collection. In most cases multipliers discriminate against high masses so that the net effect of multiplier and source tend to cancel as indicated by the results in column two. Comparison with Nier's results show that the net discrimination is almost negligible, and this is particularly so over small mass ranges. Table III gives the fission yields of xenon for two samples as measured with the multiplier and single collecting 180° instrument.

TABLE III

Fission Yields of Xenon

	131	132	134	136
Sample I.	Percent Abundances			
Multiplier	13.8 ± .02	20.4 ± .03	35.6 ± .02	30.2 ± .02
180°	13.1 ± .02	19.7 ± .02	36.2 ± .03	30.9 ± .03
Sample II.	Fission Yields (%)			
Multiplier	3.28	4.89 ± .02	8.93 ± .02	7.02 ± .02
180°	3.28	4.91 ± .02	8.98 ± .02	7.08 ± .02

The agreement between the two instruments is fairly good considering that the method of collecting is entirely different. The day to day reproducibility is indicated by the small errors.

Bohemian Pitchblende. The volume of gas extracted from the Bohemian sample was of the order of 0.01 cmm. and the fission pattern could only be measured by employing an electron multiplier. Extractions were made from two samples of ore and seven separate analyses were performed on each fraction. The results which are listed in Table IV have been calculated by arbitrarily assigning a yield of 6.5% to Xe^{136} which is based on a 3.0% yield of I^{131} in U^{235} fission.

TABLE IV

Fission Yields of Bohemian Pitchblende

	131	132	134	136
Fission Yields (%)	1.94 ± .14	4.62 ± .25	6.03 ± .09	6.50

The samples were found to contain about 80% normal xenon so that a large correction was necessary. In normal xenon, Xe^{129} is quite abundant while in fission the 129 mass chain has a low yield. The combination of these facts made it impossible to obtain an accurate value for the Xe^{129} yield since the fission component accounted for less than 1% of the observed peak. Generally Xe^{130} is used to correct for normal xenon, however, since Xe^{129} is six times as abundant and as the fission contribution was small, it was advantageous to use the 129 peak for the correction factor.

The krypton fission yields for uranium ores are usual-

ly a factor of five less than the corresponding xenon yields. The natural abundance of krypton is twenty times that of xenon so that the presence of normal rare gases make the determination of krypton yields very difficult. In the case of the Bohemian sample, the krypton fission yields amounted to 0.25% of the observed krypton peaks. Therefore it was impossible to obtain any results in this mass range.

If the only two processes involved in natural fission are $U^{235} + n$ and spontaneous fission of U^{238}, then the fission yields found for any pitchblende should be between the U^{235} and U^{238} results.

TABLE V

Sample	$U^{235} + n$	Bohemian	Belgian Congo	Spontaneous U^{238} fission
Age X 10^6 yrs.		200	640	
Fission Yields (%)				
131	3.28	1.94 ± .14	1.27 ± .04	.61 ± .01
132	4.92	4.62 ± .25	3.91 ± .06	3.74 ± .03
134	8.64	6.03 ± .09	6.03 ± .03	5.41 ± .03
136	7.10	6.50	6.50	6.50
Fine Structure (%)				
132	0	37 ± 7	40	93
134	24.5	8.5 ± 1.7	9.6	.7

The results of Table V are plotted in figure 8. The Belgian Congo yields reported by Fleming and Thode (5) showed

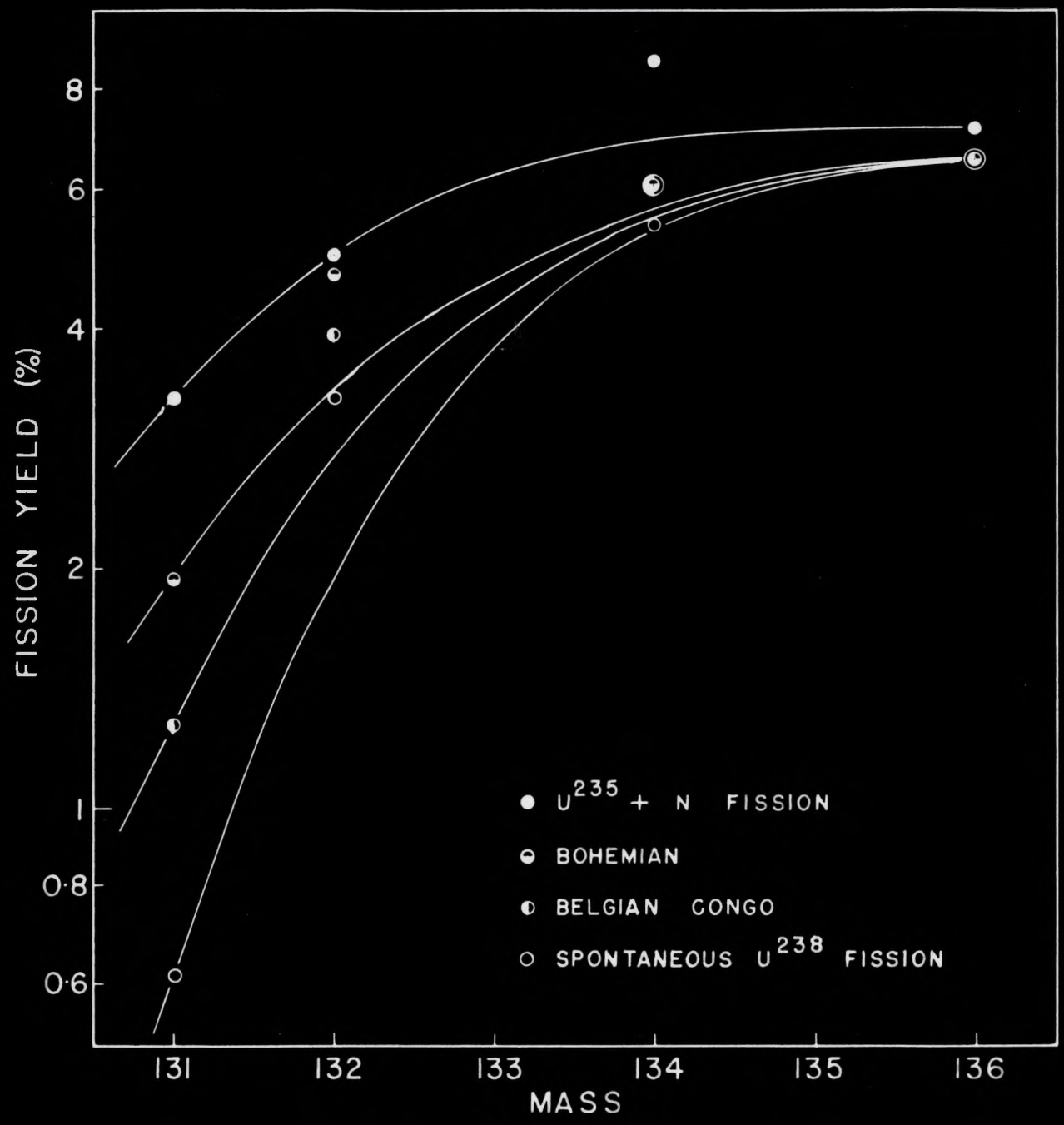

XENON YIELDS FOR NATURAL AND NEUTRON INDUCED FISSION.

FIGURE 8

about 25% neutron fission which was larger than any of the other ores analysed by them. The amount of neutron fission is characterized by the slope of the fission curve, the fine structure and the Xe^{129} yield. The slope is the most important since it represents an average of all the xenon yields while the fine structure concerns only two yields. The Bohemian sample appears to have undergone more neutron fission than the Belgian Congo ore as shown by the reduction in steepness of the fission yield curve in figure 8, and also by the fine structure. The fine structure of Xe^{132} and Xe^{134} is measured in terms of the percentage that a yield is above the smooth curve drawn through the 131 and 136 yields. Table V shows that the fine structure is shifting towards that found for U^{235} + n fission. The yields of the Bohemian ore show about equal amounts of neutron and spontaneous fission.

The large amount of neutron fission observed for the Bohemian sample would not be expected of a very young ore because of the lower U^{235}/U^{238} ratio and hence smaller chance of U^{235} + n fission. However, the results of the Belgian Congo ore which is also young suggest that some other factor carries greater influence than the age of the deposit. The concentration of the uranium minerals and the associated impurities must be of considerable importance. A sample of ore with low uranium content but in concentrated amounts would appear to favour neutron fission. Assay of the ore gives the uranium content rather than the concentration so that no quantitative estimate

can be made. The presence of rare earths in the ore which possess large neutron capture cross-sections would tend to reduce the amount of neutron fission.

In summarizing, the Bohemian pitchblende appears to have a larger neutron-to-spontaneous fission ratio than any ore previously investigated. The age of the sample indicates that the uranium ore must have been in rather concentrated amounts and that the rare earth impurities were small. The errors involved are larger than desirable, however, the high neutron fission is quite evident.

Neutron Fission of Thorium. A 5.7 gm. sample of thorium was canned in aluminium and irradiated for 6.6 months in the Los Alamos fast reactor at a flux of $5X10^{12}$ neutrons per $cm.^2$ per sec. with the most probable energy 0.5 Mev. Because of the high threshold and small cross-section for thorium fission, extremely long irradiation periods are required to produce measureable fission yields. The fission yields of the rare gases in this sample were too low to be measured accurately on a simple collecting mass spectrometer, therefore an electron multiplier was used.

Table VI lists the yields of krypton and xenon, both arbitrarily normalized to the values reported by Turkevich and Niday (9). The errors reported are the standard deviations obtained from fifteen complete spectrograms. A 50% correction was necessary for normal xenon and 20% for krypton. This contamination from normal rare gases could be reduced considerably

by improved technique.

TABLE VI

Kr and Xe Fission Yields for Thorium + n

Krypton	83	84	85	86
Yield (%)	1.90	3.40 ± .36	4.22 ± .09	6.03 ± .05
Xenon	**131**	**132**	**134**	**136**
Yield (%)	2.63 ± .24	4.25 ± .35	6.73 ± .18	6.50

Kr^{85} occurs as two isomers, one with a 10.27 year half-life and the other with a 4.4 hour half-life (25). The short lived isomer had completely decayed before the mass spectrometer studies of the fission gases were carried out, consequently the observed yields of Kr^{85} are the yields of the 10.27 year isomer only. The value given in Table VI for the 85 mass chain was calculated from the yield of the 10.27 year isomer using the fact that 22.5% of the 85 chain decays through that isomer. This figure was obtained by Bergstrom (26) and later by Wanless (25). The calculation for the yield of the 85 chain is obtained from the following relation

$$\text{total 85 yield} = \frac{\text{amount measured}}{1 - \frac{(1 - e^{-\lambda T})e^{-\lambda t}}{\lambda T}} \times .225$$

where T is the time in the pile, t the time from removal to analysis and $\lambda = \frac{0.693}{10.27}$ yrs.$^{-1}$.

TABLE VII

Krypton Yields For Various Fissioning Nuclei

Krypton Yield (%)	Th^{232} + n	U^{233} + n (27)	U^{235} + n (25)	U^{238} + n (25)	Pu^{239} + n (27)
83	1.90	1.20	0.65	0.41	0.080
84	3.40 ± .36	1.99	1.22	0.85	0.127
85	4.22 ± .09	2.63	1.55	0.65	0.200
86	6.03 ± .05	3.37	2.41	1.37	0.211

The krypton yields listed in Table VII are plotted in figure 9. If a straight line is arbitrarily drawn through the 83 and 86 yields then the 84 and 85 yields do not lie on the line. In every case the 84 yield appears high while the 85 yield is low for U^{238}, normal for U^{235} and high for Th^{232}, U^{233} and Pu^{239}. The graph shows the dependence of fine structure on the fissioning nucleus and also that an increase in the 85 mass chain is accompanied by a decrease of the 84 mass chain. This fact suggests some connection between the two chains.

To explain fine structure it is necessary to consider both prompt and delayed neutrons and also the favouring of certain masses in the primary fission process. Fleming (27) has suggested that the fine structure in the krypton range can be satisfactorily explained by assuming that a 0.43 second delayed neutron activity found in uranium fission is associated with

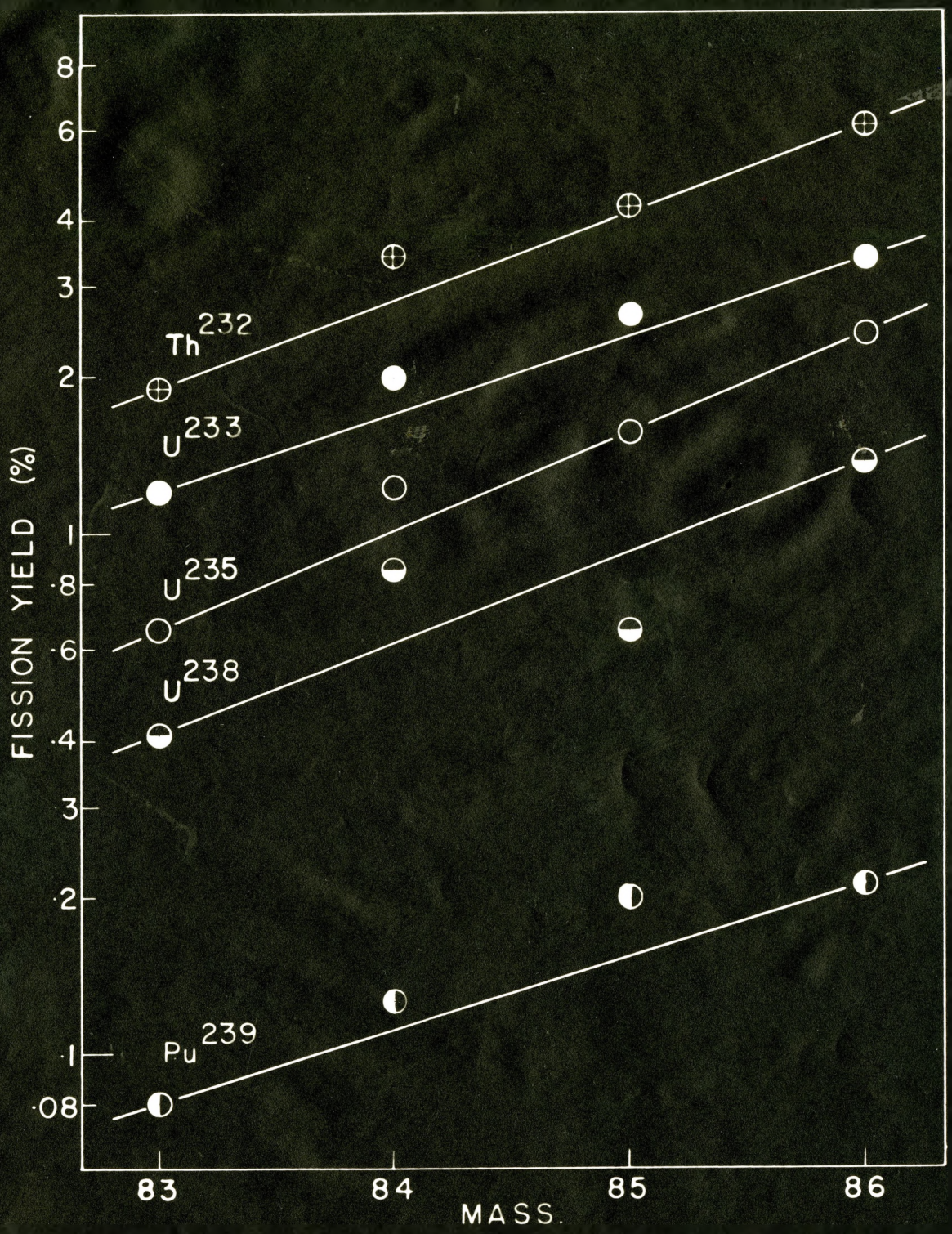

FISSION YIELDS OF KRYPTON

FIGURE 9

As^{85}[†]. The reaction can be represented by the equation

$$\left[As^{85}\right]^{*} \rightarrow As^{85} + n + Q$$

and the cumulative yield of As^{85} can be calculated on the basis of the theory of equal charge displacement. A primary fission preference for the 85 mass chain is also assumed and good agreement with experiment is possible provided the 0.43 second activity is that of As^{85}.

The calculations involved for the delayed neutron effect are shown in Table VIII. The value for the total 85 mass chain yield was obtained by taking the yield from the smooth curve in figure 9 and increasing it by 20% because of the proposed primary fission preference of the 85 chain. The most probable charge Z_p and the cumulative yield of As^{85} are calculated according to the findings of Pappas (11). The branching ratio of 21.9% was obtained by finding the cumulative yield for As^{85} in U^{235} + n fission and determining the value necessary for a 0.21% delayed neutron activity. Assuming the branching ratio of 21.9% remains independent of the fissioning nucleus, the loss from the 85 chain can be calculated.

The agreement is well within the experimental error as shown in Table VIII. A preference for the 85 mass chain

---

[†] The 0.43 second activity amounts to 0.21% in U^{235} + n fission (28).

TABLE VIII

Delayed Neutron Emission of As^{85}

	Mass 84	Mass 85
Smooth curve yield (%)	2.78	4.10
20% preference for 85 chain		4.10 X 1.2 = 4.92
Z_p for mass number 85		33.1
Cumulative yield of As^{85}		3.51
Loss from 85 chain		3.51 X .219 = .77
Predicted yields (%)	2.78 + .77 = 3.55	4.92 - .77 = 4.15
Observed yields (%)	3.40 ± .36	4.20 ± .09

implies a high yield for the complementary mass of 144 or 145 depending on the number of neutrons emitted. The results of Turkevich indicate a high yield for 144 although the errors are too large to reach any quantitative conclusion.

The position of the low mass hump has been found to depend on the fissioning nucleus which is shown by the relative yield of the curves in figure 9.

The assumption that the fission yield curve is a straight line in the krypton region appears valid for heavier fissioning nuclei, however this would not necessarily seem the case for U^{233} and Th^{232} since the krypton range is approaching the peak of the curve. The most probable heavy and light mass for Th^{232} is 140 and 91. The smooth curve values of Kr^{86} and Xe^{135} which are both six mass units from the peak are 6.03

and 6.04% respectively. This implies that the outside parts of the fission curve fall away more rapidly than the valley sides in the range of yields greater than 1%.

The xenon yields which are shown in figure 10 are similar to the curves found for U^{235}, U^{238} and Pu^{239}. Fine structure is apparent at Xe^{132} and Xe^{134} while Xe^{131} and Xe^{136} yields have been assumed to fall on the smooth radio chemical curve. Although the fission yield curve for Th^{232} is not too accurately known, the four yields do not lie on a smooth curve regardless of the normalization. A good method for comparing fine structure is to consider the ratio of observed yield to the smooth curve yield since this is independent of the normalization. The values for these ratios are given in Table IX.

TABLE IX

Nuclei	Th^{232}	U^{235}	U^{238}	Pu^{239}
A/Z	2.58	2.56	2.59	2.54
Ratio for 132	1.11	1.13	1.12	1.11
Ratio for 134	1.23	1.50	1.22	1.29
Most probable Heavy mass (9)	140	138	140	138
Most probable Light mass(9)	91	97	98	99

The Th^{232} fine structure is most similar to U^{238} as would be expected since their A/Z values, which determines Z_p, are almost the same.

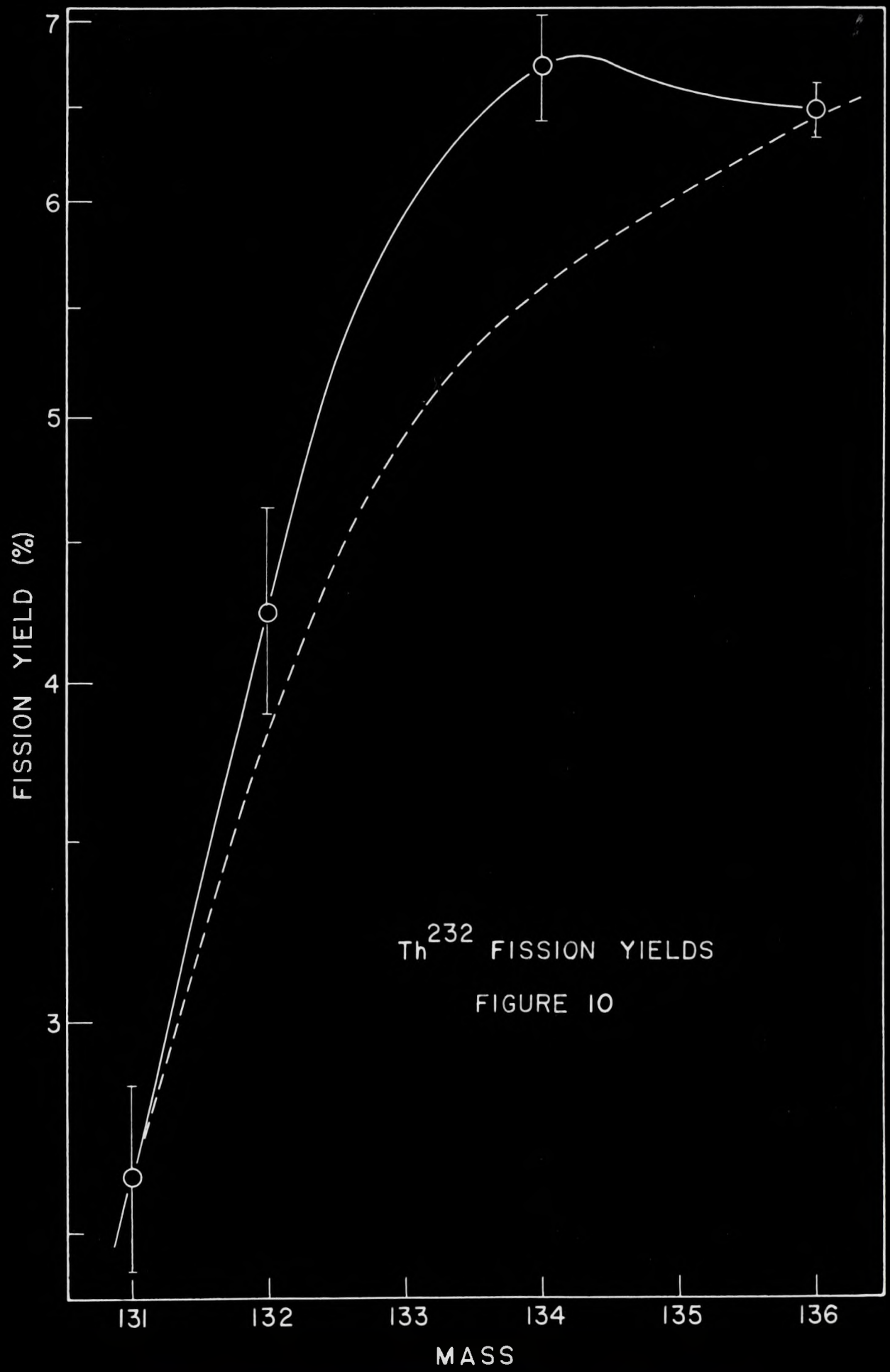

Th^{232} FISSION YIELDS

FIGURE 10

If all the mass yields in the xenon region were known it might be possible to obtain some quantitative figures on the fission preference for certain mass chains. However, the fact that the yields for masses 133 and 135 are not known prevents the development of a scheme similar to that used for the krypton region.

The smooth mass yield curve in figure 10 is much steeper than the corresponding ones for plutonium and the isotopes of uranium. This implies that there is a shift of the high mass hump to larger masses which is in agreement with the results listed in Table IX. The most probable heavy mass appears to depend on the A/Z value of the fissioning nucleus while the light mass depends on the mass of the fissioning nucleus.

BIBLIOGRAPHY

1. Flerov, G. N., and Petrzhak, K. A., Phys. Rev. 58:89. 1940.

2. Segre, E., Los Alamos Scientific Report LACD-975, 1945.

3. Macnamara, J., and Thode, H. G., Phys. Rev. 80:471. 1950.

4. Glendenin, L. E., Phys. Rev. 75:337. 1949.

5. Fleming, W. H., and Thode, H. G., Phys. Rev. 92:378. 1953.

6. Wetherill, G. W., Phys. Rev. 92:907. 1953.

7. Hahn, O., and Strassmann, F., Naturwissenschaften 27:11. 1939.

8. Haxby, Shoupp, Stephens, and Wells, Phys. Rev. 57:1088. 1940.

9. Turkevich, A., and Niday, J., Phys. Rev. 84:52. 1951.

10. Glendenin, L. E., M.I.T. Laboratory for Nuclear Science Technical Report No. 35. 1949.

11. Pappas, A. C., M.I.T. Laboratory for Nuclear Science, Technical Report No. 65. 1953.

12. Bohr, N., and Wheeler, J. A., Phys. Rev. 56:426. 1939.

13. Coryell, C. D., Ann. Rev. Nuclear Sci. 2:305. 1953.

14. Healea, M., and Chaffee, E., Phys. Rev. 49:925. 1936.

15. Allen, J. S., Phys. Rev. 55:336. 1939.

16. Allen, J. S., Phys. Rev. 55:966. 1939.

17. Cohen, A., Phys. Rev. 63:219. 1943.

18. Inghram, M., and Hayden, R., Handbook of Mass Spectroscopy, April 1952.

19. Allen, J. S., R.S.I. 18:739. 1947.

20. Allen, J.S., Proc. of I.R.E. Vol. 38 No. 4. Apr. 1950.

21. Stone, R. P., R.S.I. 20:935. 1949.

22. Inghram, M., Private communication with H.G. Thode, Oct., 1951.

23. Nier, A. O., Phys. Rev. 79:450. 1950.

24. Arrol, Chackett, and Epstein, Can. J. of Research 27B:757. 1949.

25. Wanless, R.K., Ph. D. Thesis, McMaster University, 1953.

26. Bergstrom, I., M. Siegbahn Commemerative Volume XX.

27. Fleming, W. H., Ph. D. Thesis, McMaster University, 1954.

28. Hughes, D., Dabbs, J., Cahn, A., and Hall, D., Phys. Rev. 73:111. 1948.